Journal of Immunological Methods 465 (2019) 45–52

Contents lists available at ScienceDirect

Journal of Immunological Methods

journal homepage: www.elsevier.com/locate/jim

Research paper

Phage-based assay for rapid detection of bacterial pathogens in blood by Raman spectroscopy

Laura M. De Plano[a], Enza Fazio[b], Maria Giovanna Rizzo[a], Domenico Franco[b], Santina Carnazza[a], Sebastiano Trusso[c], Fortunato Neri[b], Salvatore P.P. Guglielmino[a,*]

[a] Department of Chemical, Biological, Pharmaceutical and Environmental Sciences, University of Messina, Viale F. Stagno d'Alcontres 31, 98166 Messina, Italy
[b] Department of Mathematical and Computer Sciences, Physical Sciences and Earth Sciences, University of Messina, Viale F. Stagno d'Alcontres 31, 98166 Messina, Italy
[c] IPCF-CNR Institute for Chemical-Physical Processes, Viale Ferdinando Stagno d'Alcontres 37, 98158 Messina, Italy

ARTICLE INFO

Keywords:
Phage display
M13 filamentous phage
Sepsis
Phage-capture system
Raman spectroscopy

ABSTRACT

Sepsis is a systemic inflammatory response ensuing from presence and persistence of microorganisms in the bloodstream. The possibility to identify them at low concentrations may improve the problem of human health and therapeutic outcomes. So, sensitive and rapid diagnostic systems are essential to evaluate bacterial infections during the time, also reducing the cost. In this study, from random M13 phage display libraries, we selected phage clones that specifically bind surface of *Staphyloccocus aureus*, *Pseudomonas aeruginosa* and *Escherichia coli*. Then, commercial magnetic beads were functionalized with phage clones through covalent bond and used as capture and concentrating of pathogens from blood. We found that phage-magnetic beads complex represents a network which enables a cheap, high sensitive and specific detection of the bacteria involved in sepsis by micro-Raman spectroscopy. The enter process required 6 h and has the limit of detection of 10 Colony Forming Units on 7 ml of blood (CFU/7 ml).

1. Introduction

Sepsis is a systemic inflammatory response, characterized by hemodynamic, metabolic and inflammatory derangement, which is the result of the presence and persistence of microorganisms in the bloodstream (Polat et al., 2017). Sepsis has a high mortality risk, rapidly increasing with time in absence of optimal antibiotic therapy (Richter et al., 2018). Therefore, rapid, selective and sensitive point-of-care tools for the detection of pathogens are highly demanded in clinic diagnosis and disease control. *Staphylococcus aureus* and *Streptococcus pneumonia* are the most common Gram-positive isolates, whereas *Escherichia coli*, *Klebsiella* spp. and *Pseudomonas aeruginosa* predominate among Gram-negative isolates. Clinical laboratories adopt a two-step strategy. In the first one, an automated blood culture system detect the presence of growing organisms, thereafter species identification by genotypic and phenotypic assays is performed. However, such a procedure is time consuming and results are provided after a period of several days or weeks (Braga et al., 2013). On the contrary molecular techniques, such as real-time polymerase chain reaction (Tatavarthy and Cannons, 2010) are faster, but their use, is limited by the need of skilled operators and very expensive equipment. Moreover, isolation of microbial DNA from high concentration of blood cells, that can inhibit the dissociation of DNA polymerase, is very difficult. In recent years, optical spectroscopies, such as fluorescence or near infrared spectroscopies, were used to discriminate among different bacterial strains (Silva et al., 2014; Goldstein et al., 2018). In particular, Raman spectroscopy is an analytical technique that can detect the molecular vibrations in biological systems, such as cells and tissues (Kong et al., 2015) as well as bacteria (Huang et al., 2010; Willemse-Erix et al., 2010). However, in spite of its advantages, the major drawbacks are represented by the very low Raman cross section and by the small probed sample volume, which is a limit when the target bacterial concentration is extremely low (Lorenz et al., 2017). As a consequence separation, concentration as well as early growth on enriched medium of bacterial cells continue to be critical steps for the detection of pathogens (Stevens and Jaykus, 2004; Intra et al., 2016).

Recently, bacteria were captured by beads array, also in microfluidic devices (Hejazian et al., 2015). Beads play an important role in biosensor development since they have a three-dimensional structure with a higher surface area to volume ratio compared to a flat surface, consequently providing more binding sites for target. Another advantage is their easy manipulation in fluids in addition to a low cost also for the detection of antibodies with a low titer (Hansenová Maňásková et al., 2016; Sutarlie et al., 2016). At present, systems of

* Corresponding author.
E-mail address: sguglielm@unime.it (S.P.P. Guglielmino).

https://doi.org/10.1016/j.jim.2018.12.004
Received 24 October 2018; Received in revised form 11 December 2018; Accepted 11 December 2018
Available online 12 December 2018

magnetic-nanoparticles (MNPs) are based on immune-magnetic assay in which beads coated with bioactive molecule as antibodies, peptides, DNA are used for target identification (Waseem et al., 2014; Yang et al., 2017; Ciocchini et al., 2013). However, the use of antibodies and synthetic peptides has some disadvantages like their sensibility to physical-chemical variations of environment such as pH, temperature, mechanical stresses organic solvent, and their extremely high production and purification costs.

It is known that phage-display is a powerful tool for the isolation of peptide ligands and can be used as a good alternative of antibodies in the recognition of specific targets (Petrenko and Vodyanoy, 2003; Hu et al., 2017; De Plano et al., 2018). In our recent study, we have proposed the use of commercial magnetic or latex beads functionalized with phage clones, selective for *P. aeruginosa,* in liquid samples (Calabrese et al., 2015; Lentini et al., 2016). We demonstrated that phage probes covalently bound to beads maintain the ability to capture bacteria target in suspension.

In this study, to overcome the limits of current bacteria detection systems, a proof of concept to concentrate and rapidly detect three different microorganisms responsible for the most frequent bloodstream infections is described. The method is based on the phage display technology to be bacteria specific selective, the trapping of bacterial cells by beads and their detection and classification by Raman spectroscopy.

2. Material and methods

2.1. Bacteria and growth media

P. aeruginosa ATCC 27853 and *E. coli* LE392 (F− strain) was propagated in Luria Bertani broth (LB) and Luria Bertani Agar (LA) substrates. *Staphylococcus aureus* ATCC 29213 was propagated in Tryptone Soya Broth (TSB) and Tryptone Soya Agar (TSA) substrates. *TG1 Escherichia coli* was used for propagation of phage clones. Stock organisms were maintained in LB or TSB containing 20% (*v*/v) glycerol at −80 °C.

P9b and St.au 9IVS5 phage clones were derived from M13-pVIII-9aa phage peptide library through previously described affinity-selection procedures. These clones display the foreign peptide QRKLAAKLT and RVRSAPSSS, which represent specific and selective probes for *P. aeruginosa* (Carnazza et al., 2008) and *S. aureus* (De Plano et al., 2017), respectively. The probes specificity and selectivity were tested against different bacteria target as reported in our previous works (Carnazza et al., 2008; De Plano et al., 2017).

2.2. Phage peptide selection and specificity

The procedure described in (Carnazza et al., 2008) with minor modifications was used to isolate specific phage clone against *E. coli LE392* (F− strain). DNA sequencing and peptide analysis as well as phage capture ELISA test were carried out.

Briefly, the landscape phage library used, constructed in the vector pC89, consists of M13 phage particles that displays random 9mer peptides, fused to phage the major coat protein (pVIII). Firstly, the library was used for pre-selected with the plastic materials which will be used to the selection protocol. 10^{12} phage not binding phage clones were used for four rounds of affinity selection against *E. coli* LE392 (F− strain) whole cells (OD_{660} 0.5) in phosphate-buffered saline (PBS, 137 mM NaCl,2.7 mM KCl, 10 mM phosphate buffer, pH 7.4; 1 ml) for 60 min at room temperature (RT) with gentle agitation. Bacteria-phage complex was precipitated by spinning for 5 min at 16000 ×g, and separated from unbound phage in solution by a series of 10 washing and centrifugation steps (16,000 ×*g*, 5 min) with 1 ml TBS/Tween buffer (50 mM Tris–HCl (pH 7.5), 150 mM NaCl,0.05% (*v*/v) Tween 20) each time. Bound phage were pelleted with cells, and finally eluted with 250 µl of 0.2 M glycine–HCl (pH 2.2) by gentle shaking at RT for 20 min. Then, the solutions were neutralized with 25 µl of 1 M Tris–HCl (pH 9.1). Eluted phages from the four round of affinity selection against bacteria cells were used to infect *E. coli* TG1 cells and then these were plated on LB agar plates containing ampicillin. This was used to randomly select bacterial colonies, each containing a single selected phage, which were propagated for subsequent analyses.

To evaluate the specificity of phage clones selected performed ELISA test the procedure is: 96-Well Microplate ELISA dish (Nunc Multisorp) was coated overnight at 4 °C with 100 µl suspensions of (OD_{660} 2.0) a panel of other Gram positive, *Staphylococcus epidermidis* ATCC 12228, *Staphylococcus aureus* ATCC 29213, *Bacillus subtilis* ATCC 6633, *Listeria monocytogenes* ATCC 7644 and Gram negative bacteria *Pseudomonas aeruginosa* ATCC 27853, *Shigella flexneri* ATCC 12022, *Escherichia coli* ATCC 11303, in order to assess its selectivity and specificity of binding, washed 3 times with PBS/0.05% Tween 20 on an automatic plate washer, blocked with 5% non-fat dry milk in PBS/0.05% Tween for 2 h at 37 °C and washed again; reacted with at 100 µl ~ 10^{12} virions/ml in TBS for 2 h at RT with shaking, washed again (5 times); reacted with 100 µl of anti-M13 peroxidase conjugate antibody (Amersham Biosciences, Buckinghamshire, UK) at a dilution of 1:2500 in blocking buffer for 1 h at 37 °C, washed again(5 times); reacted with 100 µl of TMB (3,3,5,5-tetramethylbenzidine) liquid substrate system for ELISA for 45 min at RT and stopped with 100 µl of 1 M H_2SO_4. Wells were then read on a kinetic plate reader at 405 nm (Multiskan Reader, LabSystem).

pC89 phage vector (without recombinant insert) was used as negative control for evaluation of background from non-specific binding.

Phage DNAs, for PCR and sequencing, were derived from colonies of infected bacteria. The sequencing primers M13–40 reverse(5′- GTTTT CCCAGTCACGAC −3′) and E24 forward (5′ − GCTAC-CCTCGTTCCG ATGCTGTC −3′) were obtained from Proligo, Sigma(Milan, Italy). 1 µl of the suspended colony was added to the PCR reaction tube, containing 49 µl of the following PCR mix-ture: 10 × Mg free reaction buffer (Euro Clone, Milan, Italy) (5vol); 50 mM MgCl2(Euro Clone) (5 vol); Euro-Taq DNA polymerase(5 units l − 1Euro Clone) (0.5 vol); 2.5 mM dNTPs (Roche) (5 vol);primer M13–40 (10 pmol l − 1) (5 vol); primer E24 (10 pmol l − 1)(5 vol); doubly distilled filter-sterilized water (23.5 vol). The PCR was performed by GeneAmp PCR System 2400 (Perkin Elmer, Nor-walk, CT, USA) under the following cycling conditions: one cycle at 94 °C for 5 min; 25 cycles at 94 °C for 30 s, 52 °C for 30 s, 72 °Cfor 30 s; and one cycle at 72 °C for 7 min. The PCR products (3 µl) were analyzed by agarose gel electrophoresis (1% wt/vol agarose, Sigma, Milan, Italy) in 1 × TAE buffer. Gel was stained with ethidium bromide, illuminated on a Dark Reader, while DNA bands were visualized by a Kodak imaging system. PCR products were purified by NucleoSpin PCR Clean-up purification Kit (Macherey-Nagel)and sequenced by DNA sequencing service using the M13 primer −40.

2.3. Phage-capture ELISA (kinetic reaction)

Wells of a 96-well ELISA plates were coated overnight at 4 °C with 100 µl suspensions of bacterial strains(*P. aeruginosa* and *E. coli*) in study (OD_{660} = 1) in carbonate buffer (35 mM $NaHCO_3$, 15 mM Na_2CO_3, pH 9.6); washed 3 times with washing buffer (0.05% Tween 20 in PBS) by automatic plate washer; blocked with Blocking buffer (6% non-fat dry milk, 0.05% Tween 20 in PBS) for 2 h at 37 °C, washed again (5 times); reacted with 100 µl of specific phage clone, (P9band Li5 respectively, 10^{12} PFU/ml) at different times 15′, 30′, 1 h and 2 h at 37 °C with shaking, washed again (5 times); reacted with 100 µl of anti-M13 peroxidase conjugate antibody (Amersham Biosciences, Buckinghamshire, UK) at a dilution of 1:2500 in diluition buffer (1% non-fat dry milk, 0.05% Tween 20 in PBS) for 1 h at 37 °C, washed again (5 times); reacted with 100 µl of TMB for 45 min at room temperature and stopped with 100 µl of 1 M H_2SO_4. Optical absorbance was recorded at 450 nm (Multiscan FC).

To test *S. aureus* an ELISA kinetic reaction was performed following

the procedure reported in a previous work (De Plano et al., 2017). Briefly, a 96-Well Microplate ELISA was coated overnight at 4 °C with 100 µl suspensions of ~10^{12}virions/ml St.au9IVS5 in TBS, washed 3 times with PBS/0.05% Tween 20 on an automatic plate washer, blocked with 5% non-fat dry milk in PBS/0.05% Tween for 2 h at 37 °C and washed again (5 times); reacted with *S. aureus* ATCC 29213cells (OD_{660}2.0) 100 µl in PBS/1% non-fat dry milk +0,1% Tween20for 2 h at RT with shaking, washed again (5 times); reacted with100 µl of 1:3000 dilution of mouse anti-Lipotheicoic acid antibody(QED Biosence) for 1 h in PBS/1% non-fat dry milk +0,1% Tween20,washed again (5 times); incubated with a 1:50,000 dilution of goat anti-mouse-HRP for 1 h with shaking and washedagain (5 times); reacted with100 µl of TMB for 45 min at RT and stopped with100 µl of 1 M H_2SO_4. Wells were then read on a kinetic plate reader at 405 nm.

2.4. Phage-coated magnetic beads

The functionalization of Magnetic beads and ELISA assay on beads surface were performed so:

ScreenMAG-Amine superparamagnetic beads, with 1 µm diameter, were purchased from Chemicell GmbH (Berlin, Germany). Details of the functionalization of magnetic beads can be found in (Calabrese et al., 2015). 0.1 mg of beads was washed twice with 1 ml of 2-(N-Morpholino) EthanelSulfonic acid buffer (MES, 0.1 M pH 6.0) and resuspended in 100 µl MES + 1 mg 1-Ethyl-3[3-Dimethylaminopropyl] Carbodiimide (EDC). Phage suspensions in ultrapure water (title of $1.3{\cdot}10^{12}$PFU/ml) were added to 10^8/200 µl beads and the tubes were incubated in a rotator per 2 h at RT, with the ratio about 360 phage clones/beads. Beads were washed three times with Phosphate Buffer Saline (PBS, 0.1 M pH 7.1) and resuspended in PBS + 4% Bovine Serum Albumin (BSA) in order to block any residual uncovered sites on their surface. As storage solution PBS + 0.1% BSA + 0.05% sodium azide (NaN_3) was used. For the functionalization we used the specific selective clones to bacteria targets and the uncoated beads as a negative control (blank) for evaluation of a background signal from non-specific binding. In order to verify phage coating of the beads, we performed an ELISA assay. 20 µl of phage-functionalized beads (non-diluted and diluted 1:5 in PBS) and 20 µl of the respective negative controls, were normalized by Optical Density at 620 nm (OD620) measurement and washed three times with Washing Buffer (PBS + 0.05% Tween 20). 250 µl of anti-M13 major coat protein PVIII-HRP monoclonal conjugate (1:2500) were added. After 1 h of incubation at 37 °C and three washing steps, reactions were developed with 250 µl TMB, for 20 min in the dark, stopped with HCl 2 N and read at 450 nm in Multiscan FC.

2.5. Optimization of capture efficiency using M13 phage-coated beads

The capture ability of phage-coated beads was performed in 7 ml of artificially infected blood, captures efficiency was assessed by Standard Plate Count. In details, tests were performed by incubating 20 µl of M13phage-coated beads with bacteria target (*Pseudomonas aeruginosa ATCC 27853, Staphylococcus aureus ATCC 29213 or E. coli* LE392) for 15 min at RT on a rotator mixer. Dilutions ranging from 10^6 to 10^2 beads/7 ml of each phage-coated bead complex was evaluated in capture-testing *vs* ten-fold bacterial dilutions ranging from 10^4 to 10 cells/ml; after incubation, the beads were separated from the mixture using a magnetic-particle concentrator (DynalMPCs-S, Invitrogen Dynal AS, Oslo, Norway). Then phage-beads-captured bacteria were resuspended in PBS. Colony Forming Units per ml(CFU/ml) values were determined before and after beads incubation with bacteria and the capture efficiency percentage was calculated by spread on Agar plates, followed by incubation overnight at 37 °C. A capture test was performed with not functionalized beads (Blank). All tests were performed in triplicate and overall results are reported as mean capture percentage. For the assessment of the efficiency of the phage-magnetic separation we used the following relation:

$$Efficiency = X_{b1} + 3S_{b1}$$

where $X_{b1}$and $3S_{b1}$are the mean concentration of the blank and the standard deviation of the blank, respectively (Shrivastava and Gupta, 2011).

After the magnetic separation the complexes (phage-beads-captured/bacteria-captured) were incubated with 1 ml Mueller Hinton Broth (MHB) for 4 h at 37 °C in agitation. After, phage coated beads were removed and bacteria centrifuged at 8000 ×*g* 10 min and resuspended in 10 µl PBS buffer and dropped on to CaF_2 glass over an area of ~1 cm^2. All experiments were conducted in triplicate.

2.6. Raman spectroscopy analysis

Raman scattering was excited by the 532 nm (2.33 eV) radiation of a diode laser and analyzed by a Horiba XploRa micro-Raman apparatus equipped with an imaging flat field monochromator for use with a CCD camera detector cooled at 77 K and a full optical microscope so that users can also see their samples. An acquisition time of 100 s allowed a good signal/noise (S/N) ratio. Also, in this case, to ensure reproducibility, experiments were performed in triplicate. Multivariate data analyses were carried out with Matlab software. See more details in Ref. (Lentini et al., 2015; Lentini et al., 2016). To improve Raman analysis, all the spectra were previously subjected to some data treatment. First of all, a continuous baseline correction was performed using the adaptive iteratively re-weighted penalized least square algorithm (airPLS) (Zhang et al., 2010). Corrected spectra were then normalized to their own maximum intensity and slightly smoothed using the Savitzky-Golay smoothing-derivative procedure (Savitzky and Golay, 1964). The resulting spectra were loaded into rows of a matrix which was used as input for Principal Component Analysis (PCA) and subsequent Hierarchical Cluster Analysis (HCA). The detection by micro-Raman spectroscopy of the bacteria captured by phage magnetic separation (at different concentrations in blood samples) allowed the determination of the limit of detection (LOD).

3. Results

3.1. Phage peptide selection and specificity

We used 9-mer random M13 phage display library, containing random nonapeptides, to select the phages that bound to cell surface epitopes of *E.coli F-* strain.

E. coli F- was used to overcame the concept of the “natural specify” of the M13 bacteriophage, whose infection mechanism starts when the minor coat protein pIII attaches to the receptor present on the *F* pilus of the *E.coli* bacterium. Taking into account that no affinity for the pili of *F-* cells was demonstrable (Valentine et al., 1969), we chosen *E. coli F-* strain that does not present pilus, to determine the phage clone able to bind bacteria target in a region common to the both the type of the strains, *i.e.* with and without pilus.

After selection, individual phage clones were randomly selected from the eluted phage population and independently propagated for further screening. The most reactive individual phage clone for *E. coli F-* was Li5 (amino acid sequence: RKILRAGPL). To determine the recognition specificity of this clone, we investigated the ability of Li5 to interact preferentially with *E. coli*, respect to other potential targets (Fig. 1). The clone Li5 is found to interact more efficiently (roughly a factor 4) with *E. coli F-* and *E. coli* ATCC 11303 targets with respect to the other tested gram positive or gram negative bacteria (Fig. 1).

3.2. Phage-capture ELISA (kinetic reaction)

To evaluate the times of interaction between phage clones and the respective bacteria target, a kinetic phage-ELISA assay was performed. Both phage clones St.au9IVS5 and P9b showed a similar behavior with

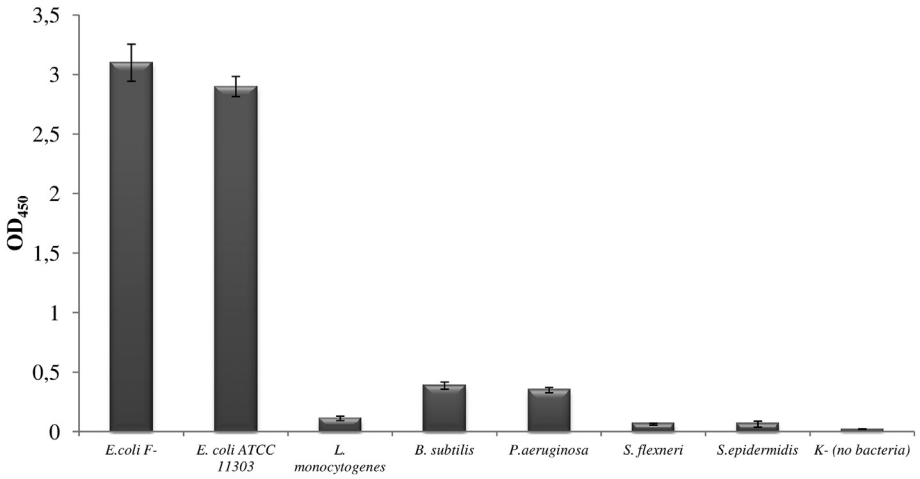

Fig. 1. Selectivity of Li5 phage as determined by ELISA test. Bacteria strains were coated on ELISA plate wells and incubated with phage clone. Mean OD_{450} is the average of three separate experiments. Error bars indicate standard deviations. Paired *t*-test indicates an extremely significant difference ($P < .0001$) for Li5 binding to *E. coli* strains with reference to all the other challenge bacteria.

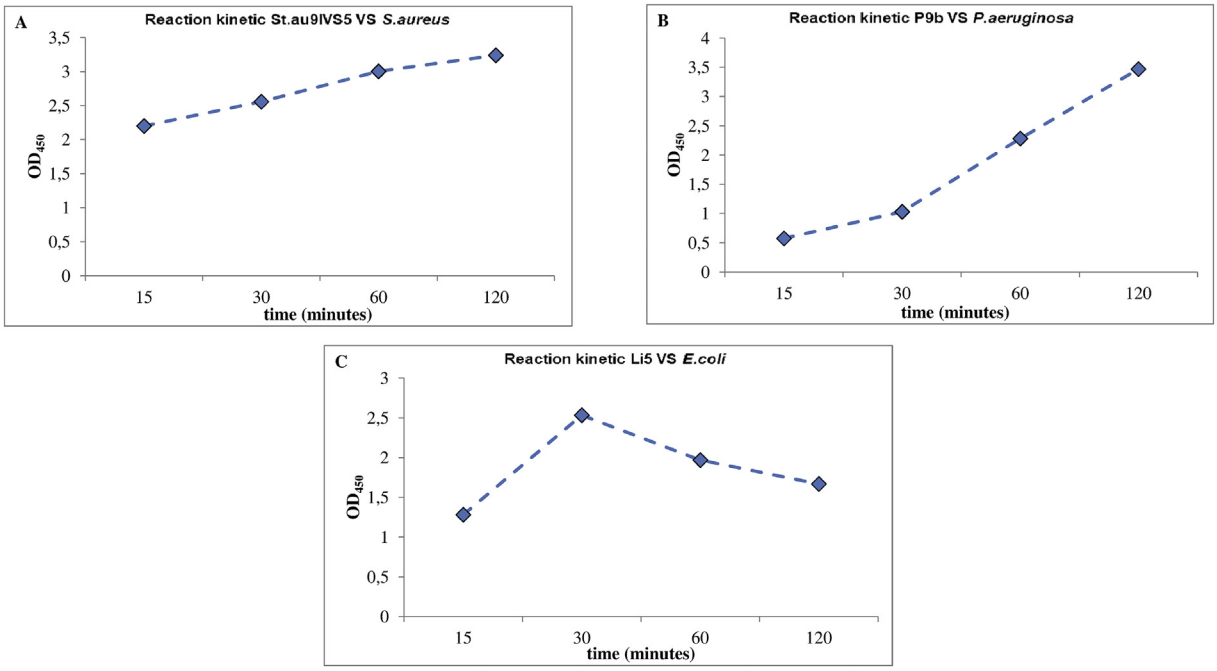

Fig. 2. Kinetic phage-capture ELISA results with the specific phage clone against bacterium target.

an initial bound at 15 min increasing with the incubation time (Fig. 2A, B). Clone Li5, able to bind and capture the specific target *E. coli*, showed a different trend, interaction with the target is observed to increase in the first 30 min, thereafter the interaction decreases (Fig. 2C).

A) St.au9IVS5 clone against *S.aureus*ATCC 29,213; B) P9b clone against *P.aeruginosa*ATCC 27,853; C) Li5 clone against *E. coli* LE392 (F− strain).Mean $OD_{450}$is the average of three separate experiments with multiple cultures. Each test was conducted at four different times15′, 30′, 1 h and 2 h at 37 °C with shaking.

3.3. Phage-coated magnetic beads

The phage clones were used to functionalize magnetic beads (screenMAG) for a magnetic separation system. In a previous work, we estimated that the best ratio for optimal functionalization of 1 μm diameter magnetic bead was 168 M13 phage clones (PFU) (Foddai et al., 2010). Phage coverage of the magnetic beads was verified by ELISA assay (Fig. 3).

3.4. Optimization of capture efficiency using M13 phage-coated beads

Fig. 4 showed the trend in a phage magnetic separation of three bacteria used in the proposed system.

It is possible observed that, using 10^2 phage-coated beads the capture efficiency resulted lower compared to tests with 10^4 and 10^6 phage-coated beads, for all the three phage clones used in the system. Instead, 10^4 phage-coated beads with St.au 9IVS5 captured 60% of bacteria targets. Similar and/or higher percentages were obtained when using 10^6 St.au9IVS5-coated beads. Consequently 10^4 St.au9IVS5-coated beads were considered the optimal concentration to capture *S. aureus* bacteria in the blood solution. The best P9b-coated beads concentration resulted 10^6, with a maximum of 70% of captured *P. aeruginosa*, respect to lower P9b-coated beads concentrations. Likewise, 10^6 Li5-coated beads showed the highest efficiency in the capture of *E. coli* with the value of 69%. Moreover, the results clearly show that uncoated beads recover a media percentage around 5–10% of bacteria target, and that this interaction is probably due to electrostatic bonds or van der Waals like forces, as reported by other author (Foddai et al., 2010). The comparison of the capture tests between phage coated beads and the

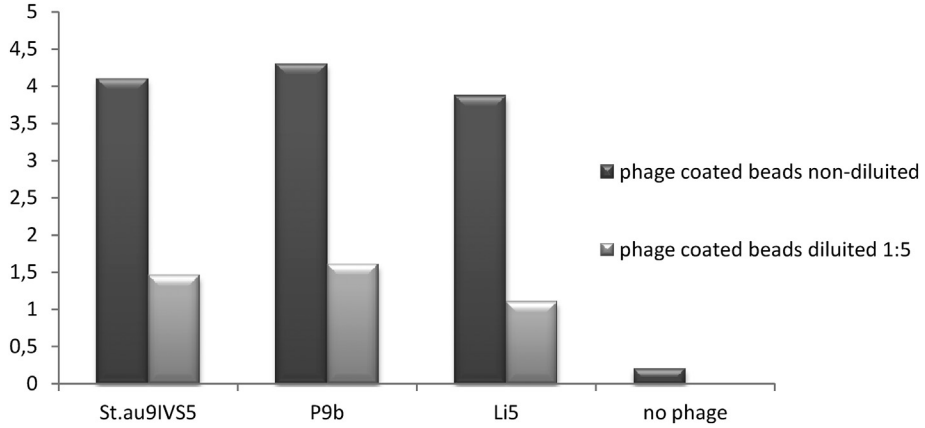

Fig. 3. ELISA assay on phage-coated beads. Target bacteria (*S. aureus, P. aeruginosa* and *E.coli*) were coated on ELISA plate wells and incubated with their specific phage clones (St.au9IVS5, P9b and Li5, respectively). Mean OD_{450} is the average of three separate experiments. Error bars indicate standard deviations.

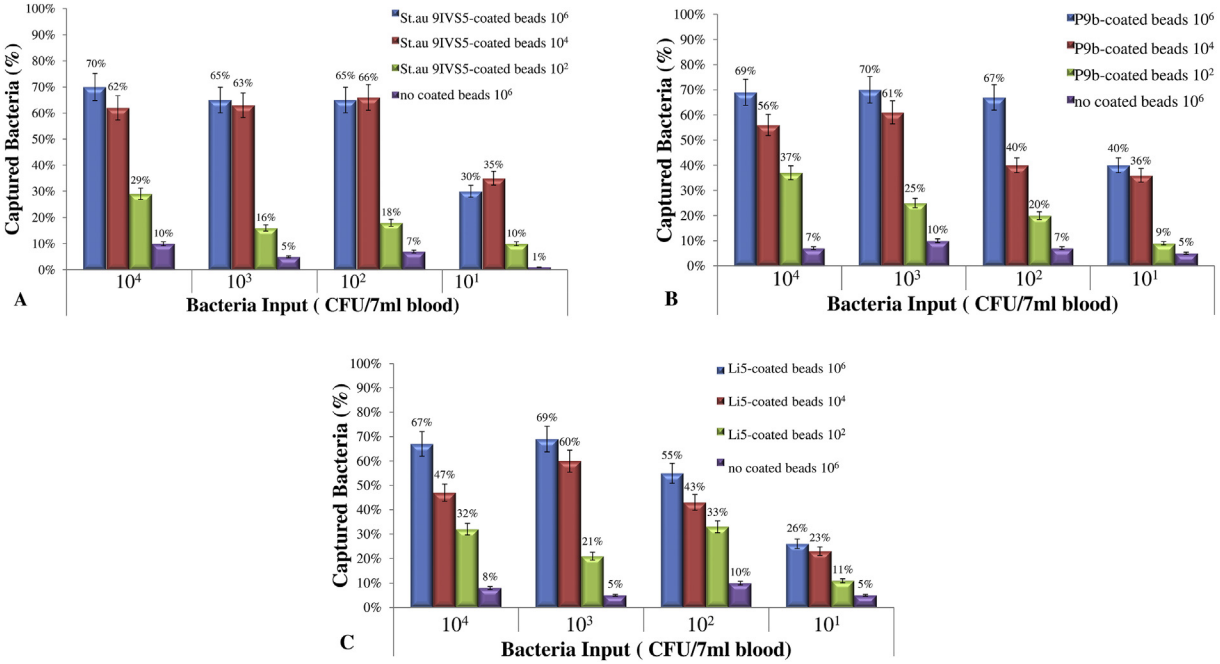

Fig. 4. Capture efficiency of phage-coated beads, with the specific phage clone, in capture test against bacterium target. A) St.au9IVS5 clone against *S. aureus*; B) P9b clone against *P. aeruginosa*; C) Li5 clone against *E. coli F-*. Mean OD_{450} is the average of three separate experiments with multiple cultures.

uncoated beads then allows to evaluate system capture efficiency at 10 CFU/7 ml, when was used the optimal concentration of each phage coated beads.

When all the phage-coated beads were dispersed in the same solution, we did not observe any negative interaction among the different phage-coated beads, a decrease, in fact, lower than 3% in the capture efficiency was observed (data not show).

3.5. Raman spectroscopy analysis

The complexes of bacteria bind to magnetic particle were incubated in rich-medium for 4 h at 37 °C in agitation. Then, bacteria were concentrated in 10 µl PBS and deposited onto a slide for micro-Raman spectroscopy measurements. In Fig. 5 are shown Raman spectra of all the investigated bacteria and PC1 and PC2 behavior as a function of wavenumber in order to remark the spectral differences for selected regions and, in turn, in relation to specific biomarkers changes (Strola et al., 2014; Kusić et al., 2014).

Details of the vibrational modes and their assignments are reported in Table 1 (Chan et al., 2006; Cheng et al., 2005; Shetty et al., 2006; Kast et al., 2008; Stone et al., 2004).

Twenty-four spectra by *E. coli* (7), *S. aureus* (8), *P. aeruginosa* (9) were collected and Raman spectra, after baseline subtraction, area normalization and smoothing procedures, were used as an input set for PCA and HCA procedures (Fig. 6A and B). From the results it can be seen as more than the 95% of the variance is within the first two principal components (PC1 and PC2).

4. Discussion

In this work we propose an alternative diagnostic tool to detect the bacteria involved in a different disease. It is known that the whole engineered bacteriophages are more stable, robust and resistant to hard pH conditions and temperature variations (Liébana et al., 2013; He et al., 2017; Ozalp et al., 2014) in comparison with peptide, antibody or aptamer to isolate the pathogen bacteria (Ozalp et al., 2014; Morton et al., 2013). So, P9b and St.au9IVS5 were used to bind *P. aeruginosa* and *S. aureus* respectively and select a specific phage clone, Li5, able to

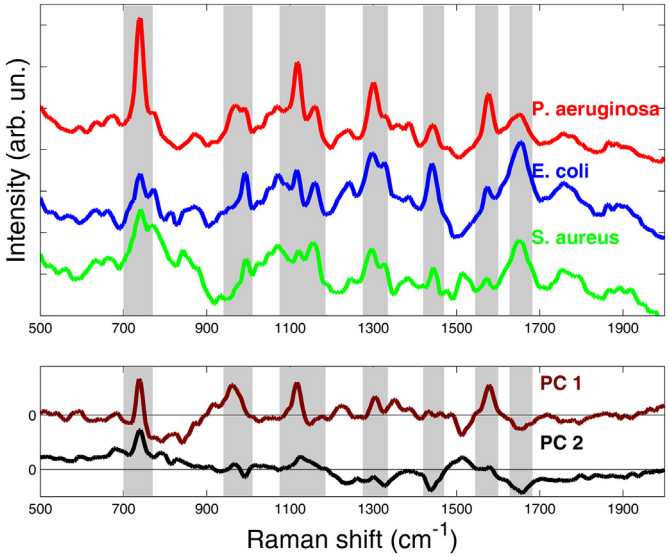

Fig. 5. Representative micro-Raman spectra of *S. aureus* (blue line), *P. aeruginosa* (violet line) and *E. coli* (green line). The shaded area that encloses each curve represents the standard deviation values limits, while the gray bands highlight the main vibrational contributions due to proteins, lipids and nucleic acids (upper panel); PC1 and PC2 as a function of wavenumber (lower panel). (For interpretation of the references to colour in this figure legend, the reader is referred to the web version of this article.)

bind *E. coli* strains (Fig. 1). We observed that all clones efficiently bound the bacteria target just after 15 min (Fig. 2A, B, C). Consequently, we performed a phage magnetic capture in one-step of 15 min and observed that the covalent bound between magnetic beads and phage clones do not compromise the peptide ability to bind the target cells (Fig. 4). According to Liébana et al., the counted colony number was found to be in all cases under 10% of the expected amount, perhaps due to the formation of probable aggregates formed by several bacterium cells but growing at a unique colony point in the agar plate (Liébana et al., 2013). Probably a single magnetic particle was able to bind to more than one bacterium and at the same time some aggregates were due to the binding of two or more magnetic particles to a single bacterium cell.

We notice that 60–70% range is the maximum percentage of bacteria capture to the phage magnetic system (Fig. 4). Sure the capture efficiency was influenced of the probability meeting between phage-coated beads and bacteria targets. As a consequence the relative amount of bacteria and beads in the solution plays an important role in the collision frequency between the two. Such optimal ratio was evaluated comparing the results using uncoated beads, and considered as negative control. The lowest cell concentration captured of phage magnetic system was 10 CFU/7 ml when was used 10^4 St.au9IVS5-coated beads to capture *S. aureus* cells and 10^6 phages coated beads to capture *P. aeruginosa* and *E.coli,* functionalized with their specific phages clone, P9b and Li5 respectively. The phage magnetic separation allows to concentrate and separate a small number of bacterial cells from blood sample and other non-target species (for example, red blood cells and albumin) present in the blood sample. This permits the successive efficient detection by micro-Raman spectroscopy (Fig. 5). In fact, Raman spectra by each bacterial species contain important information about the complex structure of the investigated cell. Particularly, the wave number regions, inked in Fig. 5 by light gray, show interesting vibrational features mostly due to proteins (amide I, II, III), aromatic amino acids (phenylalanine (Phe)) and nucleic acid components (guanine (G), adenine (A)).

In the 1500–1550 cm^{-1} spectral region, Raman signal of proteins and relevant bacteria matrix components could be also influenced by the interaction with the carotenoids (Jehlicka et al., 2013), whose main skeletal features are: C═C stretching centred at around 1520 cm^{-1}, C−C stretching around 1150 cm^{-1} and C═CH bending around 1000 cm^{-1}.

Because of the complexity of the spectra, the use of computational platforms, described in Methods section, have been required in order to easily visualize difference between bacterial species. Specifically, pre-treated spectra from considered bacteria has been used as an input set for the principal component analysis (PCA) procedure. Then, hierarchical cluster algorithm (HCA) was applied to the PCA results in order to identify statistically similar groups (see Fig. 6A and B). HCA output show that bacteria were exactly clustered into three different groups, also highlighting some existing intra-species subgroups, probably due to a different metabolic state within the same cell population (Kloß et al., 2013; Münchberg et al., 2014).

5. Conclusion

The combination of magnetic separation by M13-phage-coated beads and micro-Raman spectroscopy allow to capture, concentrate and rapidly detect different bacterial strains present in a biological sample. This efficient phage-separation consents to concentrate a few number of pathogens, an essential step to diagnose sepsis at the very beginning of a bacterial infection; moreover permit isolation of the microorganisms from complex biological samples, improves the subsequent identification analyses. Differences in the features of Raman spectra of different microorganism can be recognized by PCA and HCA statistical tools. The proposed methodology is faster, inexpensive and shows comparable sensitivity with respect to others methods. In fact, the process requires a maximum of 6 h and has a LOD of 10 CFU in 7 ml for each tested bacteria.

The proposed system is an alternative diagnostic tool for detecting and monitoring of bacterial agents in various applications including clinical based diagnostics and food. Moreover, the system organized with phage as probes could be is extensible and applicable to detection of other bacteria.

Author contributions

L.M.D.P., M.G. R. performed phage display screening and validated the *E. coli* -binding peptide; L.M.D.P., D.F. and S.C. optimized coupling

Table 1
Raman band used as molecular species-specific fingerprint, corresponding vibrational modes and their assignments. ν stretching mode; δ, bending mode.

Raman band (cm^{-1})	Vibrational modes	Assignments	References
710–760	Symmetric ring breathing mode	DNA/RNA bases; Protein	(Chan et al., 2006; Cheng et al., 2005)
940–1010	Skeletal modes; Symmetric ring breathing mode	Lipid; Protein	(Cheng et al., 2005; Shetty et al., 2006)
1070–1170	ν(C−C) or ν(C−O); C−C, C−N stretching	Lipid; Protein	(Chan et al., 2006; Kast et al., 2008)
1270–1320	Amide III; CH_2 deformation	Protein; Lipid	(Stone et al., 2004)
1420–1450	Ring breathing modes; δ(CH_2), δ(CH_3)	DNA/RNA bases; Lipid	(Chan et al., 2006; Kast et al., 2008)
1500–1550	(C−C AND C═C) stretching modes and C═CH bending modes	Carotenoids	(Jehlicka et al., 2013)
1550–1600	C═C stretching; Symmetric ring breathing mode	Protein; DNA bases	(Chan et al., 2006; Cheng et al., 2005)
1630–1670	Amide I; C═C stretching	Protein; Lipid	(Cheng et al., 2005; Stone et al., 2004)

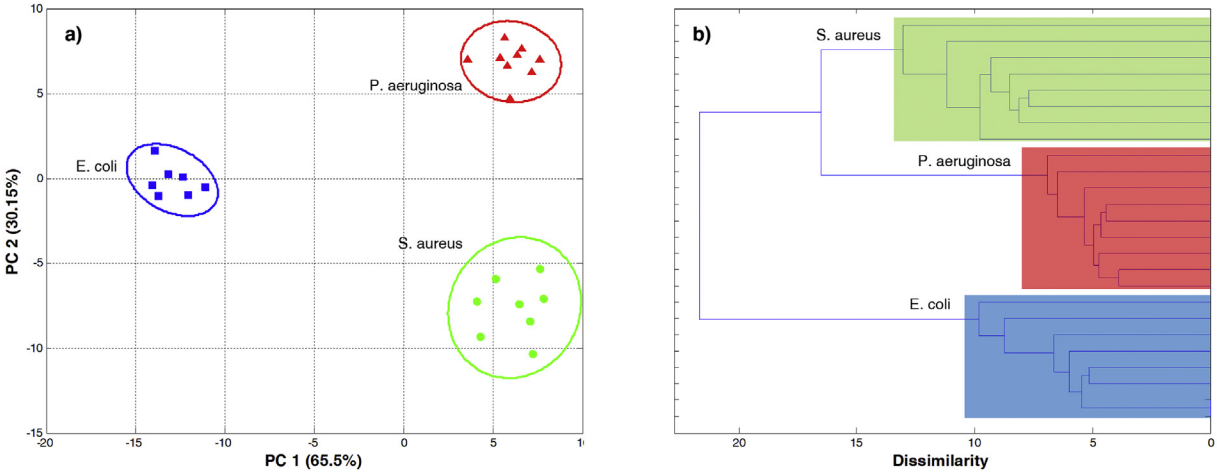

Fig. 6. Output by PCA (A) and HCA (B) analysis of bacterial spectra. The points enclosed in the ellipses and the different colour (blue, red and green) refer to the clusters, as they were identified by the HCA algorithm. Spectra input, from each bacterium strain, are indentified by different symbols (square for *E. coli*, circle for *S. aureus* and triangle for *P. aeruginosa*) in the PCA graph. (For interpretation of the references to colour in this figure legend, the reader is referred to the web version of this article.)

phage-magnetic beads, performed *in vitro* experiments. E.F and F.N performed Raman spectroscopy analysis, S.T performed statistical analysis of Raman data and S.P.P.G. discussed and analyzed data, conceived the project, and wrote the manuscript.All authors read and approved the manuscript.

Funding

This work was funded by Italian Ministry of Education, University and Research (MIUR) by means of the national Program PONR&C 2007–2013, project “Hippocrates–Sviluppo di Micro e Nano-Tecnologie e Sistemi Avanzati per la Salute dell'uomo (PON02 00355)”.

Conflicts of interest

All other authors have no conflicts of interest to declare.

Acknowledgements

Authors acknowledge financial support of A.B. A.L. onlus Messina (Italy) for XploRA Raman spectrometer use and the kind gift of phage-display libraries from Prof. Felici.

References

Braga, P.A.C., Tata, A., dos Santos, V.G., Barreiro, J.R., Schwab, N.V., dos Santos, M.V., Eberlina, M.N., Ferreira, C.R., 2013. Bacterial identification: from the agar plate to the mass spectrometer. RSC Adv. 3, 994–1008. https://doi.org/10.1039/c2ra22063f.

Calabrese, F., Carnazza, S., De Plano, L.M., Lentini, G., Franco, D., Guglielmino, S.P.P., 2015. Phage-coated paramagnetic beads as selective and specific capture system for biosensor applications. In: XVIII AISEM Annual Conference, https://doi.org/10.1109/AISEM.2015.7066851.

Carnazza, S., Foti, C., Gioffrè, G., Felici, F., Guglielmino, S.P.P., 2008. Specific and selective probes for Pseudomonas aeruginosa from phage-displayed random peptide libraries. Biosens. Bioelectron. 23 (7), 1137–1144. https://doi.org/10.1016/j.bios.2007.11.001.

Chan, J.W., Taylor, D.S., Zwerdling, T., Lane, S.T., Ihara, K., Huser, T., 2006. Micro-Raman spectroscopy detects individual neoplastic and normal hematopoietic cells. Biophys. J. 90 (2), 648–656. https://doi.org/10.1529/biophysj.105.066761.

Cheng, W.T., Liu, M.T., Liu, H.N., Lin, S.Y., 2005. Micro-Raman spectroscopy used to identify and grade human skin pilomatrixoma. Micrsc. Res. Tech. 68, 75–79. https://doi.org/10.1002/jemt.20229.

Ciocchini, A.E., Rey Serantes, D.A., Melli, L.J., Iwashkiw, J.A., Deodato, B., Wallach, J., Feldman, M.F., Ugalde, J.E., Comerci, D.J., 2013. Development and validation of a novel diagnostic test for human brucellosis using a glyco-engineered antigen coupled to magnetic beads. PLoS Negl. Trop. Dis. 7 (2), e2048. https://doi.org/10.1371/journal.pntd.0002048.

De Plano, L.M., Carnazza, S., Messina, G.M.L., Rizzo, M.G., Marletta, G., Guglielmino, S.P.P., 2017. Specific and selective probes for Staphylococcus aureus from phage-displayed random peptide libraries. Colloids Surf. B Biointerf. 157, 473–480. https://doi.org/10.1016/j.colsurfb.2017.05.081.

De Plano, L.M., Scibilia, S., Rizzo, M.G., Crea, S., Franco, D., Mezzasalma, A.M., Guglielmino, S.P.P., 2018. One-step production of phage–silicon nanoparticles by PLAL as fluorescent nanoprobes for cell identification. Appl. Phys. A 124, 222. https://doi.org/10.1007/s00339-018-1637-y.

Foddai, A., Elliott, C.T., Grant, I.R., 2010. Maximizing capture efficiency and specificity of magnetic separation for Mycobacterium avium subsp. paratuberculosis cells. Appl. Environ. Microbiol. 76 (22), 7550–7558. https://doi.org/10.1128/AEM.01432-10.

Goldstein, S.D., Beaulieu, R.J., Niño, D.F., Chun, Y., Banerjee, A., Sodhi, C.P., Hackam, D.J., 2018. Early detection of necrotizing enterocolitis using broadband optical spectroscopy. J. Pediatr. Surg. 53 (6), 1192–1196. https://doi.org/10.1016/j.jpedsurg.2018.02.083.

Hansenová Maňásková, S., van Belkum, A., Endtz, H.P., Bikker, F.J., Veerman, E.C., van Wamel, W.J., 2016. Comparison of non-magnetic and magnetic beads in bead-based assays. J. Immunol. Methods 436, 29–33. https://doi.org/10.1016/j.jim.2016.06.003.

He, Y., Wang, M., Fan, E., Ouyang, H., Yue, H., Su, X., Liao, G., Wang, L., Lu, S., Fu, Z., 2017. Highly specific bacteriophage-affinity strategy for rapid separation and sensitive detection of viable Pseudomonas aeruginosa. Anal. Chem. 89 (3), 1916–1921. https://doi.org/10.1021/acs.analchem.6b04389.

Hejazian, M., Li, W., Nguyen, N.T., 2015. Lab on a chip for continuous-flow magnetic cell separation. Lab Chip 15, 959. https://doi.org/10.1039/c4lc01422g.

Hu, Y.-F., Zhao, D., Yu, X.-L., Hu, Y.-L., Li, R.-C., Ge, M., Xu, T.-Q., Liu, X.B., Liao, H.-Y., 2017. Identification of bacterial surface antigens by screening peptide phage libraries using whole bacteria cell-purified antisera. Front. Microbiol. 8, 82. https://doi.org/10.3389/fmicb.2017.00082.

Huang, W.E., Li, M., Jarvis, R.M., Goodacre, R., Banwart, S.A., 2010. Shining light on the microbial world the application of Raman microspectroscopy. Adv. Appl. Microbiol. 70, 153–186. https://doi.org/10.1016/S0065-2164(10)70005-8.

Intra, J., Sala, M.R., Falbo, R., Cappellini, F., Brambilla, P., 2016. Reducing time to identification of aerobic bacteria and fastidious micro-organisms in positive blood cultures. Lett. Appl. Microbiol. 63 (6), 400–405. https://doi.org/10.1111/lam.12682.

Jehlicka, J., Edwards, H.G.M., Oren, A., 2013. Bacterioruberin and salinixanthin carotenoids of extremely halophilic Archaea and Bacteria: a Raman spectroscopic study. Spectrochim. Acta A Mol. Biomol. Spectrosc. 106, 99–103. https://doi.org/10.1016/j.saa.2012.12.081.

Kast, R.E., Serhatkulu, G.K., Cao, A., Pandya, A.K., Dai, H., Thakur, J.S., Naik, V.M., Naik, R., Klein, M.D., Auner, G.W., Rabah, R., 2008. Raman spectroscopy can differentiate malignant tumors from normal breast tissue and detect early neoplastic changes in a mouse model. Biopolymers 89, 134–241. https://doi.org/10.1002/bip.20899.

Kloß, S., Kampe, B., Sachse, S., Rösch, P., Straube, E., Pfister, W., Kiehntopf, M., Popp, J., 2013. Culture independent Raman spectroscopic identification of urinary tract infection pathogens: a proof of principle study. Anal. Chem. 85, 9610–9616. https://doi.org/10.1021/ac401806f.

Kong, K., Kendall, C., Stone, N., Notingher, I., 2015. Raman spectroscopy for medical diagnostics—from in-vitro biofluid assays to in-vivo cancer detection. Adv. Drug Deliv. Rev. 89, 121–134. https://doi.org/10.1016/j.addr.2015.03.009.

Kusić, D., Kampe, B., Rösch, P., Popp, J., 2014. Identification of water pathogens by Raman microspectroscopy. Water Res. 48, 179–189. https://doi.org/10.1016/j.watres.2013.09.030.

Lentini, G., Fazio, E., Calabrese, F., Deplano, L.M., Puliafico, M., Franco, D., Nicolò, M.S., Carnazza, S., Trusso, S., Allegra, A., Neri, F., Musolino, C., Guglielmino, S.P.P., 2015. Phage-AgNPs complex as SERS probe for U937 cell identification. Biosens. Bioelectron. 74, 398–405. https://doi.org/10.1016/j.bios.2015.05.073.

Lentini, G., Franco, D., Fazio, E., De Plano, L.M., Trusso, S., Carnazza, S., Neri, F.,

Guglielmino, S.P.P., 2016. Rapid detection of Pseudomonas aeruginosa by phage-capture system coupled with micro-Raman spectroscopy. VIBSPE 86, 1–7. https://doi.org/10.1016/j.vibspec.2016.05.003.

Liébana, S., Spricigo, D.A., Cortés, M.P., Barbé, J., Llagostera, M., Alegret, S., Pividori, M.I., 2013. Phagomagnetic separation and electrochemical magneto-genosensing of pathogenic bacteria. Anal. Chem. 85 (6), 3079–3086. https://doi.org/10.1021/ac3024944.

Lorenz, B., Wichmann, C., Stöckel, S., Rösch, P., Popp, J., 2017. Cultivation-free Raman spectroscopic investigations of bacteria. Trends Microbiol. 25 (5), 413–424. https://doi.org/10.1016/j.tim.2017.01.002.

Morton, J., Karoonuthaisiri, N., Stewart, L.D., Oplatowska, M., Elliott, C.T., Grant, I.R., 2013. Production and evaluation of the utility of novel phage display-derived peptide ligands to Salmonella spp. for magnetic separation. J. Appl. Microbiol. 115 (1), 271–281. https://doi.org/10.1111/jam.12207.

Münchberg, U., Rösch, P., Bauer, M., Popp, J., 2014. Raman spectroscopic identification of single bacterial cells under antibiotic influence. Anal. Bioanal. Chem. 406, 3041–3050. https://doi.org/10.1007/s00216-014-7747-2.

Ozalp, V.C., Bayramoglu, G., Kavruk, M., Keskin, B.B., Oktem, H.A., Arica, M.Y., 2014. Pathogen detection by core-shell type aptamer-magnetic preconcentration coupled to real-time PCR. Anal. Biochem. 447, 119–125. https://doi.org/10.1016/j.ab.2013.11.022.

Petrenko, V.A., Vodyanoy, V.J., 2003. Phage display for detection of biological threat agents. J. Microbiol. Methods 53 (2), 253–262 (12654496).

Polat, G., Ugan, R.A., Cadirci, E., Halici, Z., 2017. Sepsis and septic shock: current treatment strategies and new approaches. Eur. J. Med. 49 (1), 53–58. https://doi.org/10.5152/eurasianjmed.2017.17062.

Richter, D.C., Heininger, A., Brenner, T., Hochreiter, M., Bernhard, M., Briegel, J., Dubler, S., Grabein, B., Hecker, A., Krüger, W.A., Mayer, K., Pletz, M.W., Störzinger, D., Pinder, N., Hoppe-Tichy, T., Weiterer, S., Zimmermann, S., Brinkmann, A., Weigand, M.A., Lichtenstern, C., 2018. Bacterial sepsis: diagnostics and calculated antibiotic therapy. Anaesthesist 66 (10), 737–761. https://doi.org/10.1007/s00101-017-0363-8.

Savitzky, A., Golay, M.J.E., 1964. Smoothing and differentiation of data by simplified least squares procedures. Anal. Chem. 36, 1627–1639. https://doi.org/10.1021/ac60214a047.

Shetty, G., Kedall, C., Shepherd, N., Stone, N., Barr, H., 2006. Raman spectroscopy: elucidation of biochemical changes in carcinogenesis of oesophagus. Br. J. Cancer 94, 1460–1464. https://doi.org/10.1038/sj.bjc.6603102.

Shrivastava, A., Gupta, V.B., 2011. Methods for the determination of limit of detection and limit of quantitation of the analytical methods. Chron. Young Sci. 2 (1), 21–25. https://doi.org/10.4103/2229-5186.79345.

Silva, R.R., Avelino, K.Y.P.S., Ribeiro, K.L., Franco, O.L., Oliveira, M.D.L., Andrade, C.A.S., 2014. Optical and dielectric sensors based on antimicrobial peptides for microorganism diagnosis. Front. Microbiol. 5 (443). https://doi.org/10.3389/fmicb.2014.00443.

Stevens, K.A., Jaykus, L.A., 2004. Bacterial separation and concentration from complex sample matrices: a review. Crit. Rev. Microbiol. 30 (1), 7–24. https://doi.org/10.1080/10408410490266410.

Stone, N., Kendall, C., Smith, J., Crow, P., Barr, H., 2004. Raman spectroscopy for identification of epithelial cancers. Faraday Discuss. 126, 141–157 (PMID: 14992404).

Strola, S.A., Baritaux, J.-C., Schultz, E., Simon, A.C., Allier, C., Espagnon, I., Jary, D., Dinten, J.-M., 2014. Single bacteria identification by Raman spectroscopy. J. Biomed. Opt. 19 (11), 111610. https://doi.org/10.1117/1.JBO.19.11.111610.

Sutarlie, L., Ow, S.Y., Su, X., 2016. Nanomaterials-based biosensors for detection of microorganisms and microbial toxins. Biotechnol. J. 12 (4). https://doi.org/10.1002/biot.201500459.

Tatavarthy, A., Cannons, A., 2010. Real-time PCR detection of Salmonella species using a novel target: the outer membrane porin F gene (ompF). Lett. Appl. Microbiol. 50 (6), 645–652. https://doi.org/10.1111/j.1472-765X.2010.02848.x.

Valentine, R.C., Silverman, P.M., Ippen, K.A., Mohac, H., 1969. The F-Pilus of Escherichia coli. Adv. Microb. Physiol. 3, 1–52. doi: https://doi.org/10.1016/S0065-2911(08)60364–1.

Waseem, S., Allen, M.A., Schreier, S., Udomsangpetch, R., Bhakdi, S.C., 2014. Antibody-conjugated paramagnetic nanobeads: kinetics of bead-cell binding. Int. J. Mol. Sci. 15, 8821–8834. https://doi.org/10.3390/ijms15058821.

Willemse-Erix, D.F., Jachtenberg, J.W., Schut, T.B., van Leeuwen, W., van Belkum, A., Puppels, G., Maquelin, K., 2010. Towards Raman-based epidemiological typing of Pseudomonas aeruginosa. J. Biophotonics 3 (8–9), 506–511. https://doi.org/10.1002/jbio.201000026.

Yang, X., Zhou, X., Zhu, M., Xing, D., 2017. Sensitive detection of Listeria monocytogenes based on highly efficient enrichment with vancomycin-conjugated brush-like magnetic nano-platforms. Biosens. Bioelectron. 15 (91), 238–245. https://doi.org/10.1016/j.bios.2016.11.044.

Zhang, Z.M., Chen, S., Liang, Y.Z., 2010. Baseline correction using adaptive iteratively reweighted penalized least squares. Analyst 135, 1138–1146. https://doi.org/10.1039/b922045c.